

Cobalt Doping on Zirconium Titanate as a Potential Photocatalyst with Visible-Light-Response

Emilya Faridatul Sulaikhah, Rian Kurniawan, Mokhammad Fajar Pradipta, Wega Trisunaryanti, and Akhmad Syoufian*

Department of Chemistry, Faculty of Mathematics and Natural Sciences, Universitas Gadjah Mada, Sekip Utara, Yogyakarta 55281, Indonesia

* **Corresponding author:**

email: akhmadsyoufian@ugm.ac.id

Received: September 11, 2019

Accepted: December 16, 2019

DOI: 10.22146/ijc.49459

Abstract: Synthesis of cobalt-doped zirconium titanate (Co-doped $ZrTiO_4$) as a potential photocatalyst with visible-light-response had been conducted. Materials used in this research were titanium tetraisopropoxide (TTIP) as a precursor of TiO_2 , ZrO_2 as another semiconductor for coupling, and $CoSO_4 \cdot 7H_2O$ as the source of cobalt dopant. The composite was prepared by the sol-gel method with various cobalt contents and calcination temperatures. Composites with various Co dopant contents (0, 1, 3, 5, 7, and 9% (Co wt./Ti wt.)) were calcined at 500 °C for 4 h. In addition, the composite with 5% of dopant content was calcined at 700 and 900 °C to observe the influence of calcination temperature. All samples were characterized by using X-ray powder diffraction method (XRD), Fourier-transform infrared spectroscopy (FTIR), specular reflectance UV-Vis spectroscopy (SRUV), and scanning electron microscopy equipped with X-ray energy dispersive spectroscopy (SEM-EDS). Co-doped $ZrTiO_4$ with the lowest bandgap (2.94 eV) was achieved in a sample containing 3% of cobalt content calcined at 500 °C.

Keywords: cobalt; dopant; Co-doped $ZrTiO_4$; photocatalyst; sol-gel

■ INTRODUCTION

The increasing demand for textile products with good coloring quality makes the use of synthetic dyes in the textile industry increasing proportionally [1]. Synthetic dyes are widely used because of their better color, low prices, reusable, and various color choices [2]. Unfortunately, the use of synthetic dyes also has disadvantages, one of which can discharge waste that cannot be decomposed naturally, thus making it dangerous for the environment. Several ways for conventional textile wastewater treatment have been developed, such as chlorination, ozonation, and biodegradation. However, those methods still have several disadvantages, including high operational costs and relatively difficult to execute [3]. Therefore, one alternative for processing textile waste is to use the photocatalytic principle using a photocatalyst [4].

One of the most commonly used photocatalysts is TiO_2 . TiO_2 is a semiconductor with high photocatalytic

activity, non-toxic, relatively inexpensive, and has good stability in aqueous solutions [5]. TiO_2 is a polymorph with large bandgap values of 3.20, 3.02, and 2.96 eV for anatase, rutile, and brookite phases, respectively [6]. Anatase normally exists in the sol-gel product, while brookite is formed as a by-product of precipitation under the acidic condition at low temperature. Pure brookite has a rather difficult preparation method than anatase [7]. Among other polymorphs, anatase phase of TiO_2 is considered to exhibit the best photocatalytic activity based on the dynamics of charge carriers, chemical properties, and activity in photocatalytic degradation of organic compounds [8]. With a bandgap value of 3.20 eV, the maximum wavelength absorption of anatase is at the range of 200–400 nm, in which the UV region included. The sunlight spectrum consists of 5–7% of UV light, 46% of visible light, and 47% of infrared radiation. Therefore, modification of TiO_2 is necessary to shift the absorption to the visible-light region to increase its photocatalytic activity [9].

TiO₂ modification is performed with different methods, including by doping using transition metals [10] and coupling TiO₂ with other semiconductors [11]. TiO₂ doping with Co²⁺ transition metal has a higher photocatalytic activity than pure TiO₂ and shifts the absorption to the direction of visible light [12-13]. The higher content of the Co dopant added to TiO₂ is able to reduce bandgap value from 3.20 to 2.50 eV [14].

Zirconia (ZrO₂) has a good thermal and chemical stability, excellent strength, and high stability against photo-corrosion, thus making it a promising photocatalyst [15]. ZrO₂ coupled with TiO₂ (ZrO₂-TiO₂, ZrTiO₄) can produce a composite with higher photocatalytic activity compared to pure TiO₂, smaller bandgap than pure ZrO₂, and good thermal stability [16]. Syoufian et al. successfully synthesized photo-active zirconium titanate hollow spheres through the sol-gel method using sulfonated polystyrene as the template [17]. Doping of iron and copper into the ZrTiO₄ structure is proven to broaden its absorption spectrum onto visible region [18-19].

In this research, Co-doped ZrTiO₄ was synthesized by the sol-gel method. The sol-gel method was chosen because it offers several advantages, such as an easy process, simple equipment, homogeneous phase, the ability to control the crystal size, nano-sized powder with high purity, and low-temperature condition [20-21]. Various contents of cobalt dopant were applied to study their performance in shifting the absorption of Co-doped ZrTiO₄. Embedding the Co-doped TiO₂ on the surface of ZrO₂ was conducted to inhibit the anatase-to-rutile transformation. Higher calcination temperatures were applied to study the stability of the anatase phase under ZrO₂ presence.

■ EXPERIMENTAL SECTION

Materials

Titanium(IV) tetraisopropoxide (TTIP) (97%, Sigma-Aldrich) was used as the precursor of TiO₂. Zirconia fine powder (Jiaozuo Huasu) and cobalt(II) sulfate heptahydrate (CoSO₄·7H₂O) (Merck) were the source of ZrO₂ matrix and Co dopant, respectively. Absolute ethanol (Merck) and demineralized water (Jaya Sentosa) were chosen as solvents.

Instrumentation

The crystal structure of the material was analyzed by X-ray powder diffractometer (XRD) PANalytical X'Pert PRO MRD instrument with CuKα radiation. Fourier-Transform Infrared Spectrometer (FT-IR) analysis was conducted using Thermo Nicolet iS10. Specular Reflectance UV-Vis spectrophotometer (SRUV) UV1700 Pharmaspec was used to measure the ultraviolet and visible (UV-Vis) absorption of composites. Surface structure was observed with scanning electron microscope equipped with energy dispersive X-ray spectrometer (SEM-EDS) FlexSEM1000.

Procedure

Co-doped ZrTiO₄ was synthesized by the sol-gel method. 2.5 mL of titanium tetraisopropoxide (TTIP) precursor was dissolved in 25 mL of absolute ethanol and stirred for 30 min. 1 g of ZrO₂ powder and a certain amount of CoSO₄·7H₂O with various concentrations (0, 1, 3, 5, 7, and 9% (Co wt./Ti wt.)) were dissolved together in 25 mL of demineralized water. Diluted TTIP was added dropwise into aqueous ZrO₂-CoSO₄·7H₂O suspension. The mixture was further stirred for 30 min and separated by centrifugation at 2000 rpm for 1 h. The obtained solid was aged in the open air for 24 h and then heated at 80 °C for 24 h. Composites with various Co dopant contents were calcined at 500 °C for 4 h. The composite with 5% of dopant content was calcined at 700 and 900 °C to observe the influence of calcination temperature. All samples were characterized by using XRD, FTIR, SEM-EDS, and SRUV spectroscopy.

■ RESULTS AND DISCUSSION

Characterization of the crystalline phase was investigated by comparing the pattern of synthesized materials with references. Fig. 1 shows diffraction patterns of Co-doped ZrTiO₄ with various Co contents calcined at 500 °C. Diffraction patterns of composites show that the highest peaks belong to the two crystal phases, the anatase phase of TiO₂ and the monoclinic phase of ZrO₂. The anatase peaks were observed at 25° and 48°, while the monoclinic peaks were observed at 28° and 31°. Characteristic diffraction peaks of TiO₂ anatase

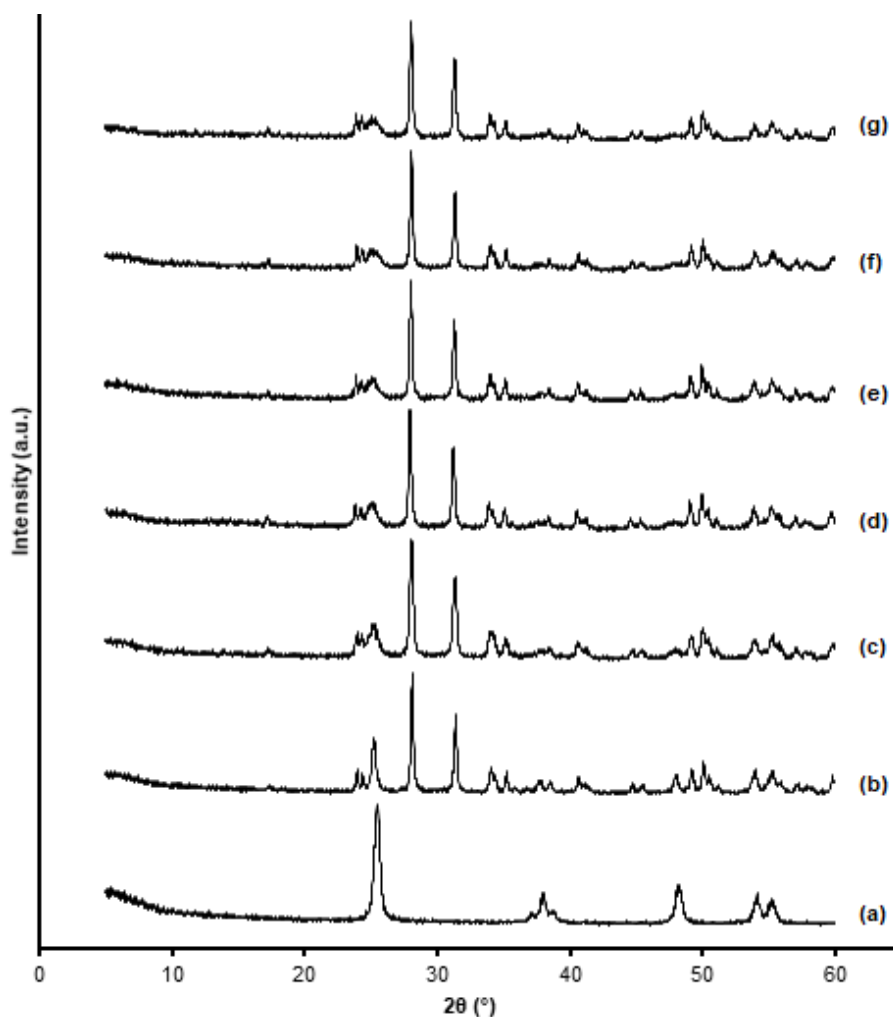


Fig 1. Diffraction patterns of (a) TiO_2 , and Co-doped ZrTiO_4 with (b) 0, (c) 1, (d) 3, (e) 5, (f) 7, and (g) 9% (Co wt./Ti wt.) of Co contents calcined at 500 °C

phase (ICDD: 00-001-0562) appear at 25° (d_{101}), 37° (d_{103}), and 48° (d_{200}). On the other hand, characteristic diffraction peaks of ZrO_2 monoclinic structure (ICDD: 00-036-0420) appear at 28° (d_{101}), 31° (d_{111}), and 34° (d_{002}). There was a decrease in the peak intensity of anatase along with an increase in Co dopant content. The higher contents of Co dopant add more Co atoms entering the crystal lattice. This causes the crystal structures to be irregular and less crystalline.

Fig. 2 shows diffraction patterns of 5% Co-doped ZrTiO_4 with various calcination temperatures and the reference material of TiO_2 calcined at 500 °C. The XRD patterns of TiO_2 and Co-doped ZrTiO_4 calcined at 500 °C show the peaks of two crystalline phases, anatase and monoclinic. The diffraction pattern of Co-doped ZrTiO_4

calcined at 700 °C shows that there was a phase transformation from anatase to rutile, as seen by the appearance of rutile peaks at 27° and 35° (ICDD: 00-004-0551; 27° (d_{110}), 36° (d_{101}), and 54° (d_{211})). The intensity of rutile patterns was higher in Co-doped ZrTiO_4 calcined at 900 °C, which corresponds with the result of previous works [18-19,22]. Anatase peak at 25° was visible with low intensity in the composites calcined at 500 and 700 °C, indicating that the presence of ZrO_2 , which is dominant as supporting material, can inhibit the anatase to rutile transformation [23].

Fig. 3 presents the FTIR spectra of Co-doped ZrTiO_4 with various Co contents and TiO_2 as a reference. All the samples were calcined at 500 °C. The results are in correspond with previous work [24], in which the

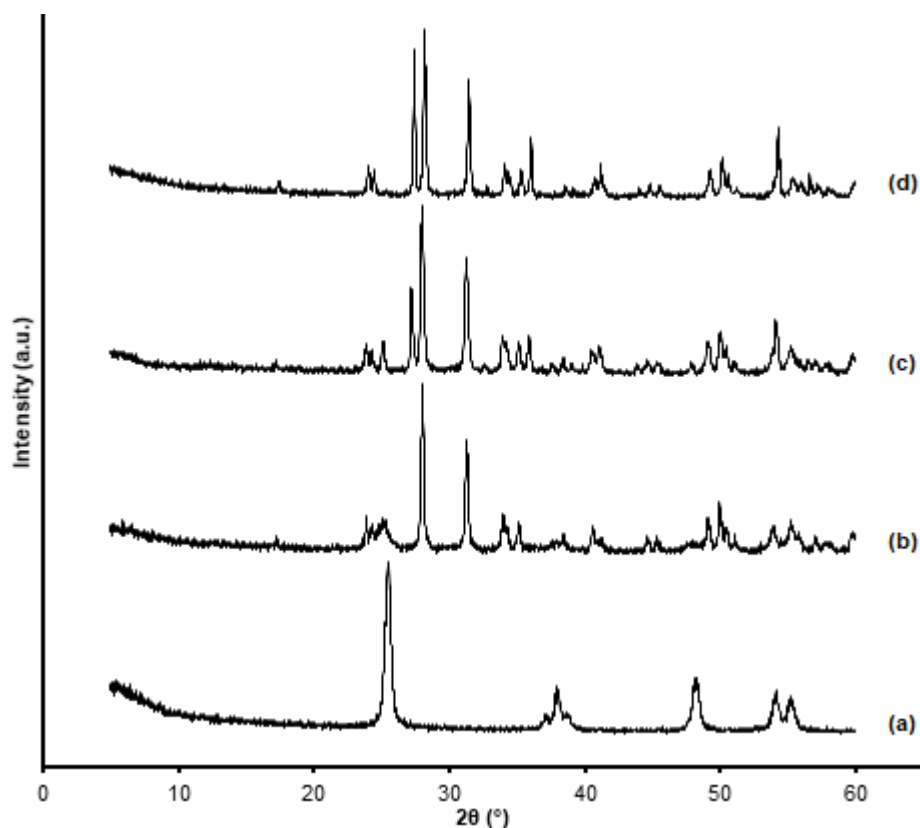


Fig 2. Diffraction patterns of (a) TiO₂ calcined at 500 °C, and 5% Co-doped ZrTiO₄ calcined at (b) 500, (c) 700, and (d) 900 °C

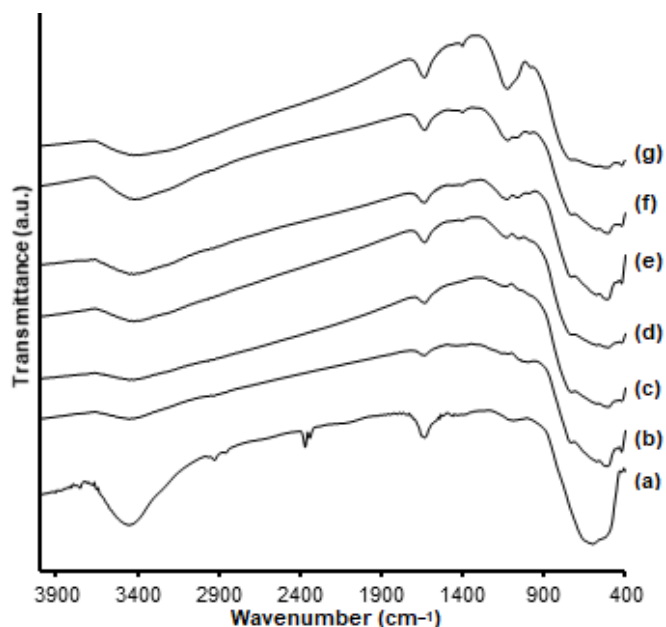


Fig 3. FTIR spectra of (a) TiO₂, and Co-doped ZrTiO₄ with (b) 0, (c) 1 (d) 3, (e) 5, (f) 7, (g) 9% (Co wt./Ti wt.) of Co contents calcined at 500 °C

absorption of the Ti–O–Ti bond at the wavenumber of 400–600 cm⁻¹ tended to weaken as the Co content increased. This indicates that cobalt had been successfully doped on composites. The Ti–O–Ti vibration is hindered by the presence of Co dopant on the ZrTiO₄ structure. Absorption at a wavenumber of 1635 cm⁻¹ shows the –OH bending vibration of H₂O, and the absorption at a wavenumber of 3300–3700 cm⁻¹ belongs to the –OH stretching vibration of H₂O. These are also in correspond with the results of previous work [25]. There was a vibrational band on Co-doped ZrTiO₄ spectra that appeared and elevated around 1100 cm⁻¹ as the cobalt content increased. The band is possibly designated to be either Co–O–Zr or Co–O–Ti vibration, or may even possibly be both.

Fig. 4 presents the FTIR spectra of 5% Co-doped ZrTiO₄ with various calcination temperatures together with TiO₂ calcined at 500 °C as reference. In general, the spectra show that composites with higher calcination

temperatures had decreasing stretching vibration of –OH ($3300\text{--}3700\text{ cm}^{-1}$) and bending vibration of H–O–H (1635 cm^{-1}) in H_2O (the intensity decreased and the peak widened). These are caused by the decrease of water content in the synthesized material due to the high heating temperature during the calcination process. The absorption of the Ti–O–Ti bond also decreased as calcination temperature increased. This is caused by the phase transformation from anatase to rutile. The bond length of the anatase phase is shorter than the rutile phase, thus resulting in different vibrational energy.

The SEM image of doped ZrTiO_4 containing 3% of cobalt content calcined at $500\text{ }^\circ\text{C}$ is shown in Fig. 5, and its corresponding EDS analysis is presented in Table 1. EDS analysis shows that the Co dopant and TiO_2 were successfully embedded on the surface of ZrO_2 . The synthesized composite appears to be in microsize with an estimated particle diameter of around $2\text{--}5\text{ }\mu\text{m}$.

Fig. 6 shows the absorption spectra of Co-doped ZrTiO_4 , whereas the corresponding bandgap values of Co-doped ZrTiO_4 are shown in Table 2. Based on the UV-Vis absorption results, turning points of synthesized materials had already at a wavelength higher than 400 nm (visible range). All synthesized composites show a lower bandgap than TiO_2 . The results are in correspond with the previous work [14], in which Co addition had succeeded in reducing the bandgap value from 3.14 eV to 2.94 eV with the optimum content of 3%. While at Co dopant contents more than 3%, the absorption edge returned to the lower wavelength. The bandgap value increased because of the diminishing doping effect and emerging heterojunction effect. The bandgap of 5% Co-doped ZrTiO_4 calcined at 700 and $900\text{ }^\circ\text{C}$ are lower than that of $500\text{ }^\circ\text{C}$. Based on the diffraction data, the rutile phase of 5% Co-doped ZrTiO_4 emerged as calcination temperature arose. Higher calcination temperatures shift the bandgap

of Co-doped ZrTiO_4 due to the higher content of the rutile phase, which has a lower bandgap than anatase. Our results show that all Co-doped ZrTiO_4 had relatively small bandgap and should be a potential photocatalyst under visible light application.

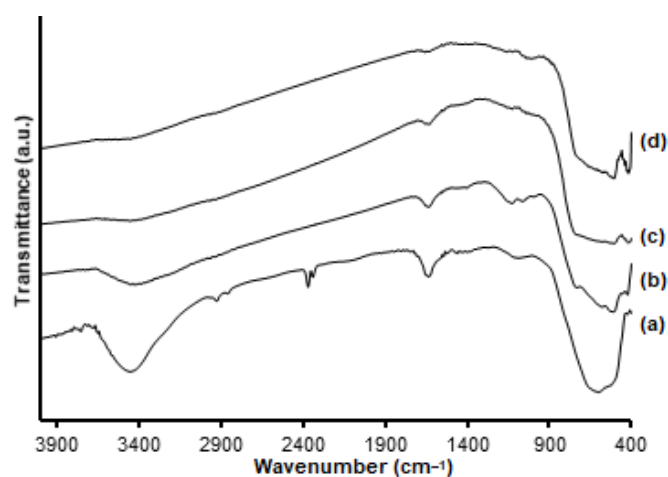


Fig 4. FTIR spectra of (a) TiO_2 calcined at $500\text{ }^\circ\text{C}$, and 5% Co-doped ZrTiO_4 calcined at (b) 500 , (c) 700 , and (d) $900\text{ }^\circ\text{C}$

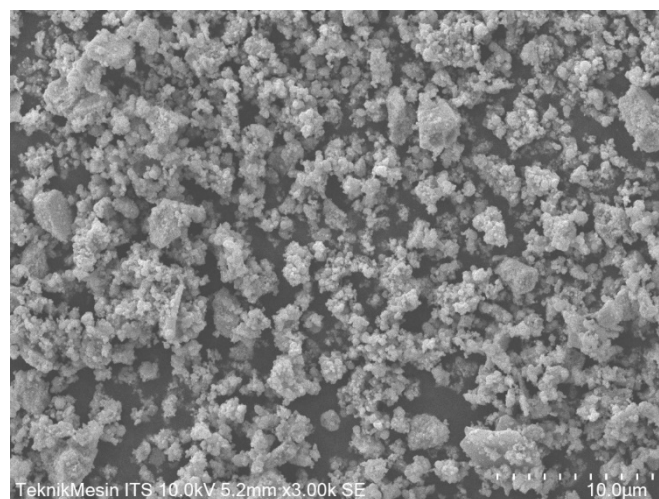


Fig 5. SEM image of 3% Co-doped ZrTiO_4 calcined at $500\text{ }^\circ\text{C}$

Table 1. EDS analysis of 3% Co-doped ZrTiO_4 calcined at $500\text{ }^\circ\text{C}$

Element	Weight %	Atomic %	Net Int.	Error %	K ratio	Z	A	F
O K	42.68	74.91	334.55	9.87	0.0629	1.1622	0.1268	1.0000
Zr L	30.22	9.30	766.97	1.12	0.2486	0.8231	0.9990	1.0012
Ti K	26.14	15.32	782.62	2.05	0.2257	0.9196	0.9301	1.0101
Co K	0.96	0.46	16.23	5.41	0.0086	0.8882	0.9616	1.0454

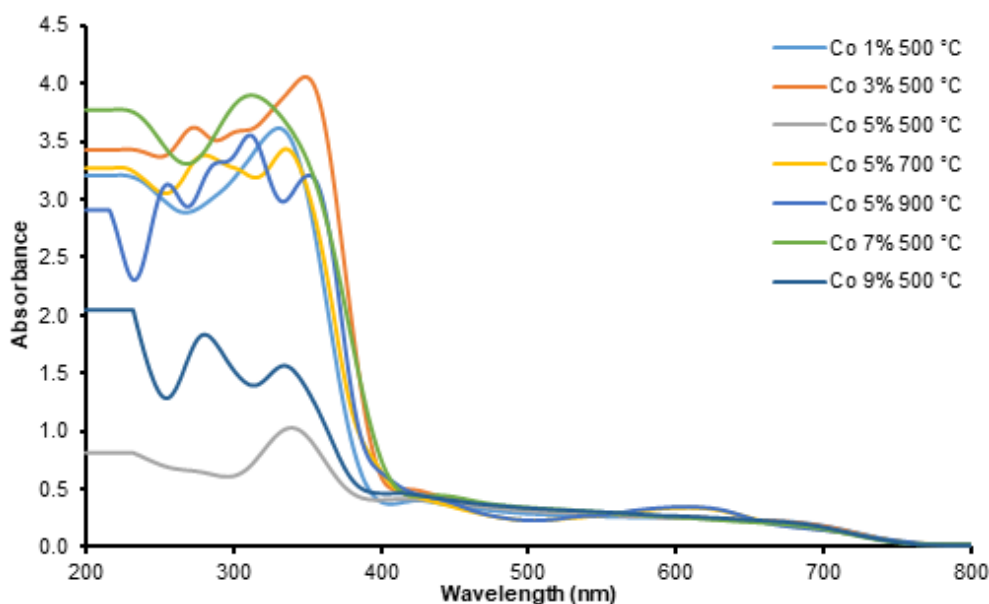


Fig 6. UV-Vis absorption spectra of various Co-doped ZrTiO₄

Table 2. Bandgap data of TiO₂ and Co-doped ZrTiO₄

Composites	E _g (eV)
TiO ₂ 500 °C	3.14
Co-ZrTiO ₄ 1% 500 °C	2.96
Co-ZrTiO ₄ 3% 500 °C	2.94
Co-ZrTiO ₄ 5% 500 °C	3.02
Co-ZrTiO ₄ 5% 700 °C	2.97
Co-ZrTiO ₄ 5% 900 °C	2.94
Co-ZrTiO ₄ 7% 500 °C	3.03
Co-ZrTiO ₄ 9% 500 °C	3.06

CONCLUSION

Synthesis of Co-doped ZrTiO₄ as a potential visible-light responsive photocatalyst by the sol-gel method had been successfully conducted. This was proved by the UV-Vis absorption spectra which show the absorption edge of composites at a wavelength more than 400 nm (visible range). The addition of Co dopants shifts the absorption of ZrTiO₄ to the visible light region. The optimum content of the Co dopant is obtained at 3% (Co wt./Ti wt.) with an optimum calcination temperature of 500 °C to give the bandgap value of 2.94 eV. The presence of ZrO₂ in composites inhibits the phase transformation of anatase to rutile at high temperatures (700 and 900 °C). All materials have displayed visible-light-response as a potential photocatalyst.

ACKNOWLEDGMENTS

We would like to express our gratitude to The Ministry of Research, Technology and Higher Education of the Republic of Indonesia for their support on this work through PDUPT 2019 Grant (2554/UN1.DITLIT/DIT-LIT/LT/2019).

REFERENCES

- [1] dos Santos, A.B., Cervantes, F.J., and van Lier, J.B., 2007, Review paper on current technologies for decolourisation of textile wastewaters: Perspectives for anaerobic biotechnology, *Bioresour. Technol.*, 98 (12), 2369–2385.
- [2] Mirjalili, M., Nazarpour, K., and Karimi, L., 2011, Eco-friendly dyeing of wool using natural dye from weld as co-partner with synthetic dye, *J. Cleaner Prod.*, 19 (9-10), 1045–1051.
- [3] Utubira, Y., Wijaya, K., Triyono, T., and Sugiharto, E., 2006, Preparation and characterization of TiO₂-zeolite and its application to degrade textile wastewater by photocatalytic method, *Indones. J. Chem.*, 6 (3), 231–237.
- [4] Alinsafi, A., Evenou, F., Abdulkarim, E.M., Pons, M.N., Zahraa, O., Benhammou, A., Yaacoubi, A., and Nejmeddine, A., 2007, Treatment of textile

- industry wastewater by supported photocatalysis, *Dyes Pigm.*, 74 (2), 439–445.
- [5] Qamar, M., Saquib, M., and Muneer, M., 2005, Photocatalytic degradation of two selected dye derivatives, chromotrope 2B and amido black 10B, in aqueous suspensions of titanium dioxide, *Dyes Pigm.*, 65 (1), 1–9.
- [6] Wunderlich, W., Oekermann, T., Miao, L., Hue, N.T., Tanemura, S., and Tanemura, M., 2004, Electronic properties of nano-porous TiO₂- and ZnO-thin films-comparison of simulations and experiments, *J. Ceram. Process. Res.*, 5 (4), 343–354.
- [7] Di Paola, A., Bellardita, M., and Palmisano, L., 2013, Brookite, the least known TiO₂ photocatalyst, *Catalysts*, 3 (1), 36–73.
- [8] Li, G., Chen, L., Graham, M.E., and Gray, K.A., 2007, A comparison of mixed phase titania photocatalysts prepared by physical and chemical methods: The importance of the solid-solid interface, *J. Mol. Catal. A: Chem.*, 275 (1-2), 30–35.
- [9] Rehman, S., Ullah, R., Butt, A.M., and Gohar, N.D., 2009, Strategies of making TiO₂ and ZnO visible light active, *J. Hazard. Mater.*, 170 (2-3), 560–569.
- [10] Huo, J., Hu, Y., Jiang, H., Hou, X., and Li, C., 2014, Continuous flame synthesis of near surface nitrogen doped TiO₂ for dye-sensitized solar cells, *Chem. Eng. J.*, 258, 163–170.
- [11] Li, Z., Wnetrzak, R., Kwapinski, W., and Leahy, J.J., 2012, Synthesis and characterization of sulfated TiO₂ nanorods and ZrO₂/TiO₂ nanocomposites for the esterification of biobased organic acid, *ACS Appl. Mater. Interfaces*, 4 (9), 4499–4505.
- [12] Siddhapara, K.S., and Shah, D.V., 2014, Study of photocatalytic activity and properties of transition metal ions doped nanocrystalline TiO₂ prepared by sol-gel method, *Adv. Mater. Sci. Eng.*, 2014, 462198.
- [13] Choi, J., Park, H., and Hoffmann, M.R., 2010, Effects of single metal-ion doping on the visible-light photoreactivity of TiO₂, *J. Phys. Chem. C*, 114 (2), 783–792.
- [14] Siddhapara, K., and Shah, D., 2012, Characterization of nanocrystalline cobalt doped TiO₂ sol-gel material, *J. Cryst. Growth*, 352 (1), 224–228.
- [15] Zhang, X., and Liu, Q., 2008, Visible-light-induced degradation of formaldehyde over titania photocatalyst co-doped with nitrogen and nickel, *Appl. Surf. Sci.*, 254 (15), 4780–4785.
- [16] Kim, J.Y., Kim, C.S., Chang, H.K., and Kim, T.O., 2011, Synthesis and characterization of N-doped TiO₂/ZrO₂ visible light photocatalysts, *Adv. Powder Technol.*, 22 (3), 443–448.
- [17] Syoufian, A., Manako, Y., and Nakashima, K., 2015, Sol-gel preparation of photoactive srilankite-type zirconium titanate hollow spheres by templating sulfonated polystyrene latex particles, *Powder Technol.*, 280, 207–210.
- [18] Andita, K.R., Kurniawan, R., and Syoufian, A., 2019, Synthesis and characterization of Cu-doped zirconium titanate as a potential visible-light responsive photocatalyst, *Indones. J. Chem.*, 19 (3), 761–766.
- [19] Kurniawan, R., Sudiono, S., Trisunaryanti, W., and Syoufian, A., 2019, Synthesis of iron-doped zirconium titanate as a potential visible-light responsive photocatalyst, *Indones. J. Chem.*, 19 (2), 454–460.
- [20] Wellia, D.V., Xu, Q.C., Sk, M.A., Lim, K.H., Lim, T.M., and Tan, T.T.Y., 2011, Experimental and theoretical studies of Fe-doped TiO₂ films prepared by peroxo sol-gel method, *Appl. Catal., A*, 401, 98–105.
- [21] Tomar, L.J., Bhatt, P.J., Desai, R.K., and Chakrabarty, B.S., 2014, Effect of preparation method on optical and structural properties of TiO₂/ZrO₂ nanocomposite, *J. Nanotechnol. Adv. Mater.*, 2 (1), 27–33.
- [22] Samet, L., Nasseur, J.B., Chtourou, R., March, K., and Stephan, O., 2013, Heat treatment effect on the physical properties of cobalt doped TiO₂ sol-gel materials, *Mater. Charact.*, 85, 1–12.
- [23] Nankya, R., and Kim, K.N., 2016, Sol-gel synthesis and characterization of Cu-TiO₂ nanoparticles with enhanced optical and photocatalytic properties, *J. Nanosci. Nanotechnol.*, 16 (11), 11631–11634.
- [24] Choudhury, B., Choudhury, A., Maidul Islam, A.K.M., Alagarsamy, P., and Mukherjee, M., 2011,

Effect of oxygen vacancy and dopant concentration on the magnetic properties of high spin Co^{2+} doped TiO_2 nanoparticles, *J. Magn. Magn. Mater.*, 323 (5), 440–446.

[25] Deng, Q.R., Xia, X.H., Guo, M.L., Gao, Y., and Shao, G., 2011, Mn-doped TiO_2 nanopowders with remarkable visible light photocatalytic activity, *Mater. Lett.*, 65 (13), 2051–2054.